Thickness effect on the tensile and dynamic mechanical properties of graphene nano-platelets reinforced polymer nanocomposites

Yu LIU, Benhui FAN, Ann-Lenaig HAMON, Delong HE, Jinbo BAI*

*Corresponding author : Tel/Fax : +33 (0)1 41 13 13 16

Email : jinbo.bai@centralesupelec.fr

Laboratoire de Mécanique des Sols, Structures et Matériaux, CentraleSupélec / CNRS UMR8579 / Université Paris-Saclay, Grande Voie des Vignes, 92290 Châtenay-Malabry, France

ABSTRACT

The thickness effect of graphene nano-platelets (GNPs) on the morphology, tensile and dynamic mechanical properties of GNPs/PMMA nanocomposites has been studied. Two types of GNPs, G5 (5nm thick) and G100 (100nm thick), were incorporated into a poly-methyl methacrylate (PMMA) matrix, each with four weight percentages: 0.1%, 0.5%, 1.0% and 5.0%. After measured by tensile test and dynamic mechanical analysis, the thinner G5 was found to improve more significantly the reinforcement of nanocomposites than G100. At 5.0wt.%, the Young's modulus of G5/PMMA was 53.6% greater than the pure PMMA as compared to a 26.1% increase for G100/PMMA; the ultimate tensile strength of G5/PMMA was enhanced by 25.5% compared to 3.1% for G100/PMMA; the storage modulus of G5/PMMA was improved by 84.3% compared to 54.1% for G100/PMMA. The fracture toughness of both nanocomposites improved greatly at 0.1wt.%: a 47.9% improvement for G5/PMMA compared with pure PMMA, and 20.8% for G100/PMMA, and maintained at the same level up to 1.0wt.%. The advantage of G5 over G100 in terms of tensile and dynamic mechanical properties enhancement was caused by its thinness, to be related to its high specific surface area.

Key words: GNPs; PMMA; Mechanical properties; Thickness effect; Nanocomposite

INTRODUCTION

With the advances in nanotechnology, nanofillers enforced polymer matrix has attracted enormous attention in the field of advanced, high performance materials since only a small loading of nanofillers in the polymer matrix can result in excellent improvements in mechanical properties [1]. A number of research groups performed studies on developing high-performance polymer composites containing nanofillers, such as alumina, carbon nanotubes, nanosilica and graphene, ranging between 0.01 and 5.0 wt.% contents, and demonstrated great improvements in tensile, flexural properties, fracture toughness, electrical and thermal properties [2-6].

Since reported, graphene has attracted considerable interest due to its outstanding physical and chemical properties [7,8]. Scientists have developed a variety range of applications for the graphene based materials, such as bio-sensors [9], super capacitors [10], drug delivery materials [11], etc. However, the expensive cost and complicated fabricating procedure have limited the wide application range of single-layer graphene. More attention have been paid on graphene nano-platelets (GNPs), a kind of carbon materials with multi-layers in structure. GNPs have similar properties to single-layer graphene but they can be readily produced in bulk quantity by means of mechanical cleavage and liquid phase exfoliation of the bulk graphite which provides more possibilities for practical applications [12,13].

Due to the two dimensional structure of GNPs, during the impregnation process of GNPs/polymer mixture, it is important to take the influence of GNPs size into account on the morphology and properties of nano-composites. Till date, a significant amount of research has been conducted in the area of graphene reinforced polymer matrix with promising outcomes. Improved fracture toughness, enhanced mechanical properties, good thermal and electrical conductivity of the modified polymers were reported by researchers [6,14,15]. However, the study of size effect, more precisely, thickness effect on the graphene/polymer nano-composites is very limited in the literatures [16].

Hence, in this work we pay attention to study the effect of GNPs with different thicknesses. We choose two kinds of GNPs, called G5 and G100, with thicknesses of 5 nm and 100nm respectively. They have been incorporated into poly-methyl methacrylate (PMMA) with four weight percentages: 0.1%, 0.5%, 1.0% and 5.0%, by solution casting and melting blending methods. Tensile test and dynamic mechanical analysis (DMA) have been conducted to evaluate the enhancement properties of two nanofillers.

EXPERIMENTAL

Preparation of GNPs/PMMA composites

The two different nanofillers, G5 and G100, were purchased from KNANO Science Inc., China and used directly without any other treatment. The procedure of preparing 0.1wt.% GNPs/PMMA composite was as follows: First, 0.02 g GNPs was dispersed in 20 mL Dimethyl Formamide (DMF, 99.8%, Sigma-Aldrich) by ultrasonics for 20min. Secondly, 19.98 g PMMA beads (melt flow index = 1.22g/min, density = 1.18, LG PMMA Corporation, Korea) was dissolved in 40 mL dimethyl formamide (DMF) solution at 100^{o}C for 2h by magnetical stirring. Then, the PMMA solution was mixed with GNPs dispersion and stirred for 30 min. Thirdly, the mixture was coated on a glass substrate and dried at 100^{o}C for 24h to evaporate the DMF solvent. In order to further process the composite, the mixture was put into a twin-screw micro-extruder/compounder (Micro 5cc Twin Screw Compounder, DSM) and blended for 20min at 220^{o}C at the speed of 60rpm. The bone-shaped 1.5mm thick slab was fabricated via the extrusion-injection method (Micro 5cc Injection Molder, DSM at 1.3MPa). The temperatures of the injection nozzle and mould holder were set at 220^{o}C and 55^{o}C, respectively. The same processes were conducted for all other composites, 0.5wt.% (0.1 g GNPs and 19.9 g PMMA), 1.0wt.% (0.2 g GNPs and 19.8 g PMMA) and 5.0wt.% (1.0 g GNPs and 19.0 g PMMA).

Characterization of the GNPs/PMMA composites

The morphology of GNPs and fracture surface of GNPs/PMMA composites was characterized by the scanning electron microscope (SEM) (Quanta 200 FEG, FEI Company) at 5 kV. Herein, composites were broken after immersion in the liquid nitrogen for 10min.

DMA was conducted in tension mode by Netzsch DMA 242C.The measurement was conducted from 30^{o}C to 150^{o}C with 2^{o}C/min heating rate at frequency of 1Hz. The size of the specimen was 12mm×5mm×1.5mm. Stress-strain curves of composites were measured by the Instron 5544 machine. The measurement was conducted by a load cell of 2kN with the cross-head speed of 2mm/min.

RESULTS AND DISCUSSION

Morphology characterization for two kinds of GNPs and fracture surfaces of GNPs/PMMA composites

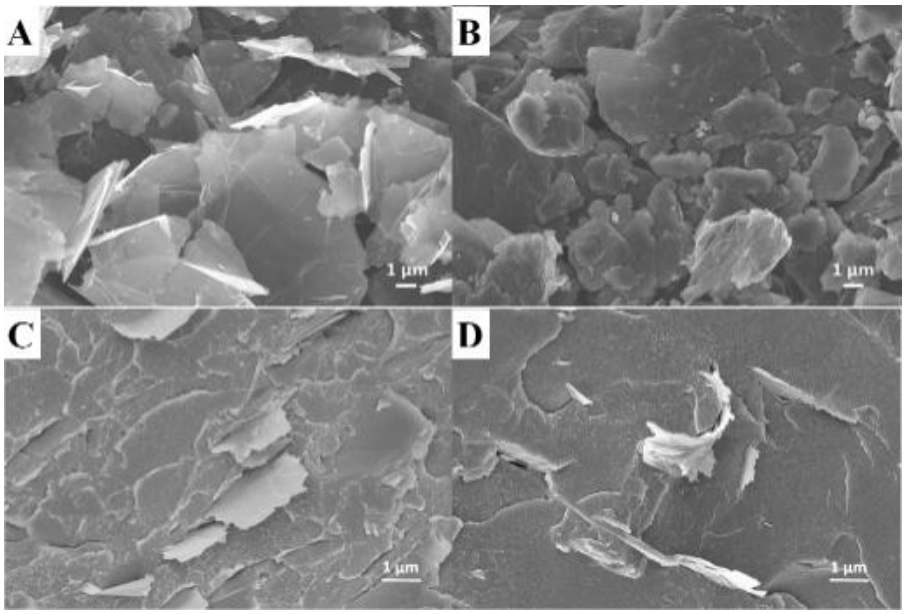

Fig 1 SEM images of G5 (A) and G100 (B) and the fracture surfaces of G5/PMMA (C) and G100/PMMA (D) composites with 5.0 wt.%.

According to the information provided by the supplier, G5 and G100 have similar diametric distribution (5-10 μm) with different thickness, 5 nm and 100 nm, respectively. Observing the SEM images of G5 (A) and G100 (B) shown in Fig 1, the difference of thickness could be figure out clearly. G5 shows semitransparent platelets in morphology which is not observed in G100. However, the diametric distribution of two GNPs could not be easily confirmed from these images. Additionally, from the information from the supplier, G5 has a much lower density than that of G100 due to its thinness.

In the SEM of G5/PMMA (C) and G100/PMMA (D) nano-composites with 5.0 wt.% shown in Fig 1, fracture surfaces of two composites are all smooth and some GNPs are pulled out directly from the PMMA matrix. It may infer that the adhesion between GNPs and PMMA is not very strong and bonded by non-covalent bond. Furthermore, it can be found that after incorporation into the polymer matrix, the GNPs are homogeneously distributed due to the solvent mixing combined with the melting blending method. However, the discrepancy in thickness for the two GNP types are not obvious, G5 seem to be much thicker than 5 nm, which indicates that aggregation still exists for the thinner GNPs. Further, it is clear from the figure that some small pieces on the G100 surface if comparing Fig 1(A) with (B). Then during the procedure of pulling out, some small pieces on G100 are stretched and rolled up from the surface, which makes it much easier to pull the platelet out from the matrix. Thus we can find in the fracture of G5/PMMA in (C), the interphase between G5

and PMMA is relatively dense and fewer cracks exist in the interface. However, in the case of G100/PMMA in (D), more cracks along the direction of platelet are formed.

Dynamic mechanical analysis for PMMA and GNPs/PMMA composites

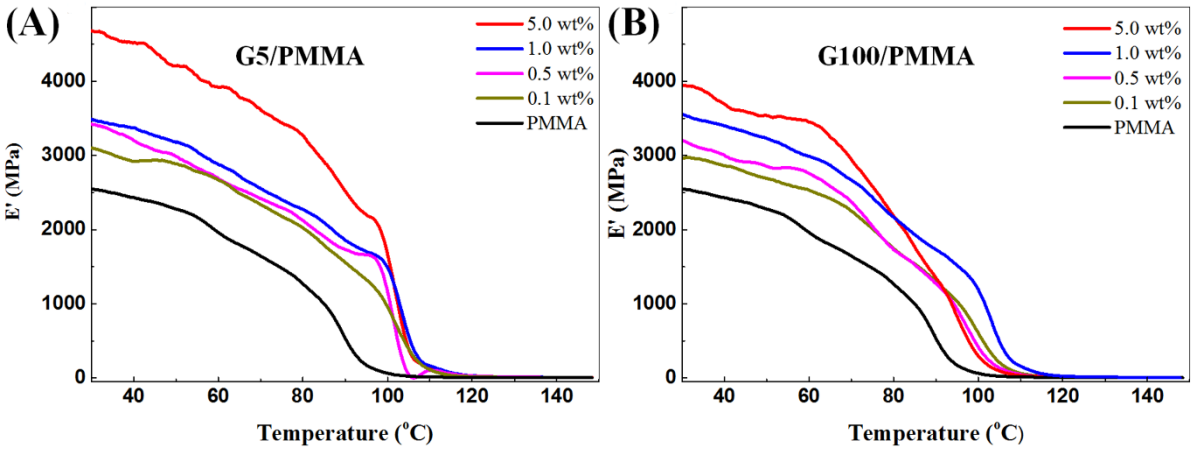

Fig 2 Temperature dependence of storage modulus for (A) G5/PMMA and (B) G100/PMMA composites with four contents: 0.1 wt.%, 0.5 wt.%, 1.0 wt.% and 5.0 wt.%, respectively.

It is known that the dynamic mechanical response of the samples is divided into two parts: the storage modulus (*E'*) and the loss modulus (*E''*).The former one is an elastic part which is related to the material stiffness and the stored energy while the later one is the viscous part which is associated with the samples ability to dissipate mechanical energy by the cycle of motion. The dynamic (complex) modulus *E** corresponds to the stress over strain ratio and is given as [17]:

$$E^* = E' + iE'' \qquad (1)$$

Comparing two graphs of temperature dependence of *E'* in GNPs/PMMA with different contents in Fig 2, it can be found that *E'* is mainly influenced by two factors: the contents of GNPs in composites and the thickness of GNPs used in composites. Furthermore, PMMA's viscoelastic behavior greatly influences *E'*. Concretely, the curves has been divided into three parts: (i) the glassy plateau (< 90 ^{o}C), (ii) the glass transition region (90-120 ^{o}C), and (iii) the leathery region (> 120 ^{o}C). In the glassy plateau range, thickness of the GNPs affects *E'* and causes drastic increase in this property compared with PMMA matrix. Concretely, the improvement on *E'* at 5.0 wt.% is 50.8% in G5/PMMA composites. However, in the case of G100/PMMA, this increase was limited to 28.9%. It is known that the storage modulus of composites is associated with the interfacial interaction between GNPs and PMMA. The different improvements in *E'* may suggest that the

interfacial interaction in the composites is affected by the thickness of the nanofillers. Hence, in the glassy plateau region, the thinner G5 may favor the interfacial interaction between GNPs and PMMA and consequently shows the higher modulus at 30°C compared with G100/PMMA composites.

Then, in the case of the glass transition region and leathery region, for the same type of GNPs, it can be found that the *E'* increases with the GNP content. For G5/PMMA composites, the *E'* value is relatively well maintained until 100°C, and then plummets to 0. However, for G100/PMMA composites, the sharp reduction in *E'* takes place near 93°C compared with G5/PMMA. Additionally, for G100/PMMA nanocomposites, there exists a slight discrepancy in the glass transition region, which is attributed to the use of solvent. Thus, the use of solvent for GNP dispersal before the melting process may affect the mechanical property of composites.

In addition, besides *E'*, *E''* values is also compared in the case of PMMA and GNP/PMMA composites. Fig 3 shows the loss modulus variation in two different nanocomposites:

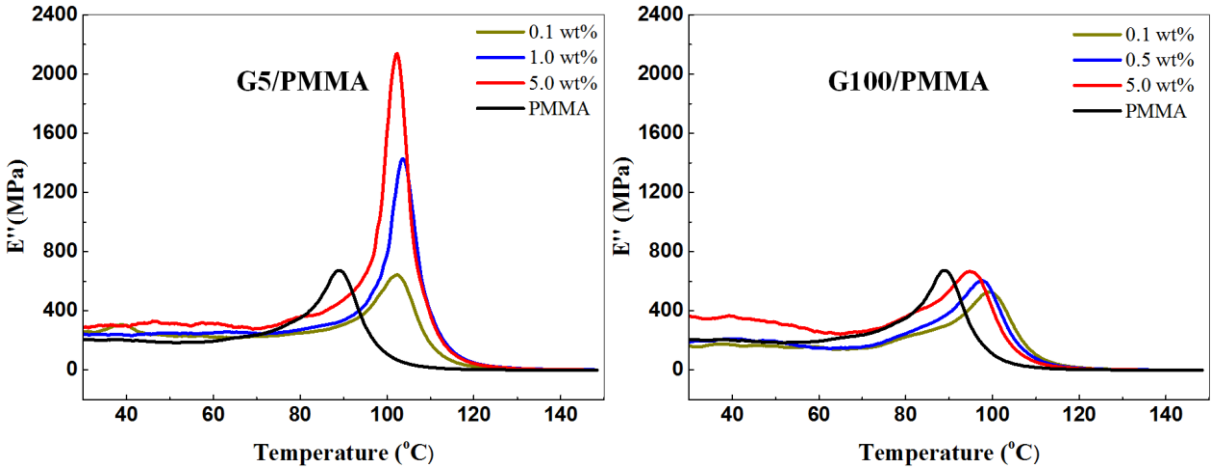

Fig 3 Temperature dependence of loss modulus *E''* for G5/PMMA and G100/PMMA composites with four contents: 0.1 wt.%, 0.5 wt.%, 1.0 wt.% and 5.0 wt.%, respectively.

In the *E''* curves, an incisive peak appears in the glass transition region and represents the complexity of a segment's motion of PMMA and the interaction between PMMA and GNPs. For G5/PMMA, the intensity of *E''* increases largely with the contents. However, the *E''* values in the case of G100/PMMA are almost at the same level as pure PMMA. These can be caused by two reasons: on the one hand, as we mentioned before, G5 has a much lower density than that of G100. Despite the total mass is the same, G5 occupies more ¨sites¨ than G100, which have larger inhibition to the segment's motion of PMMA. On the other hand, as shown in the Fig 1 (B) and (D), there are some small pieces of platelets attached on the G100's surface, during the segment motion, the interaction may locate between two layers of G100, instead of at the interface between G100 and PMMA. In

contrast, G5/PMMA has a denser interphase than G100/PMMA and better adhesion which leads to intensify *E"* in by increasing the nano contents. In addition, by comparing the value of glass transition temperature (*Tg*) in table 1, it can be found that the effect of the GNP content on *Tg* for both types of composites shows the same tendency, which increases with the contents then decreases for high concentrations. The *Tg* value here was determined by the DMA method, which greatly depended on the segment's motion. In relatively lower concentration, as the GNPs increases, the platelets in the matrix have an increased inhibition effect to the movement of polymer chains. In higher contents, due to the aggregation of nanofillers, some relative movements happen between the platelets, which serve as ¨lubricant¨ in the polymer matrix, leading to the decrease of *Tg* value. It is agreeable that the *Tg* value greatly depends on the interaction between polymer matrix and nanofillers. However, comparing with the *Tg* of pure PMMA (99.9^{o}C), in 5.0 wt.%, the nano-composites still have a much higher *Tg* value (106.8^{o}C and 107.8^{o}C, respectively).

Table 1. *Tg* values for two kinds of GNP/PMMA composites with different contents tested by DMA method.

Content	**0.1 wt.%**	**0.5 wt.%**	**1.0 wt.%**	**5.0 wt.%**
G5/PMMA	114.5°C	114.6	107.4 °C	106.8 °C
G100/PMMA	113.1°C	110.8 °C	114.9 °C	107.8 °C

Tensile measurements for PMMA and GNP/PMMA composites

The tensile measurements for PMMA and the two kinds of composites with different nanofiller contents were also conducted. The Young's modulus and strain were derived from the curves of stress-strain. For PMMA, the tested Young's modulus is 2.34GPa and its tensile strength is 53.5MPa. Fig 4 shows the normalized values:

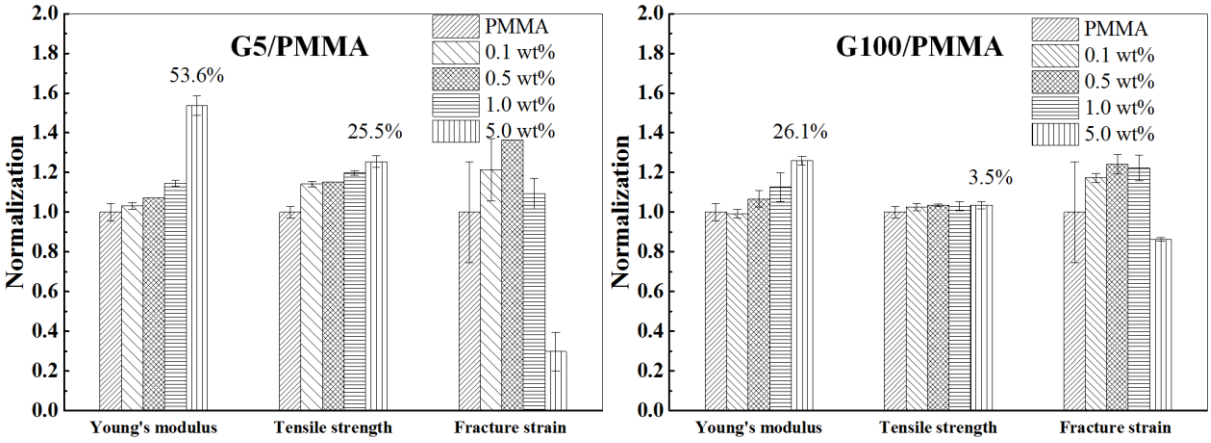

Fig 4.Mechanical properties of G5/PMMA (A) and G100/PMMA (B) calculated by stress-strain curves.

As shown in Fig 4, we can figure out that the stiffness of composites depends significantly on the GNP weight percentages. In details, the Young's modulus and tensile strength of G5/PMMA have an improvement of 53.6% and 25.5% at 5.0 wt.%, respectively. For G100/PMMA, these two values changes to 26.1% and 3.5%, respectively. Based on the Young's modulus obtained from the measurement, it is obvious that the aspect ratio of GNPs is the main cause to the variety of the mechanical properties. Comparing the data in the graph, we use the Halpin-Tsai model to predict the reinforced effect of two kinds of GNPs. The Halpin-Tsai equation is widely used to predict the tensile modulus for composites with random distributed fillers [18,19]:

$$E_c = E_m\left(\frac{3}{8}\frac{1+\eta_L\zeta V_C}{1-\eta_L V_C}+\frac{5}{8}\frac{1+2\eta_T V_C}{1-\eta_T V_C}\right) \quad (2)$$

$$\eta_L = \frac{\frac{E_g}{E_m}-1}{\frac{E_g}{E_m}+\zeta} \quad (3)$$

$$\eta_T = \frac{\frac{E_g}{E_m}-1}{\frac{E_g}{E_m}+2} \quad (4)$$

$$\zeta = k\left(\frac{T}{D}\right) \quad (5)$$

Here, E_c, E_m and Eg are the Young's modulus of the composite, PMMA (2.34 GPa) and GNP (1060 GPa), respectively. V_c is the volume fraction of GNP in the composite. For G5 and G100, we used the same density as 2.25 g/cm^3. ζ is the shape function which is associated with the aspect ratio. In light of the references [20], we set k as 2/3 for the calculation. Meanwhile, we have also defined the aspect ratio (the ratio of thickness T and diameter D of the platelet) in the SEM observation presented in section 3.1 and we will use the average value for this calculation. The comparison of experimental data and calculated data of nanocomposites is plotted in Fig 5.

From the fitting results, we find that Halpin-Tsai models can fit the experimental data well for G100/PMMA composites. But as the percentage reaches 5.0 wt.%, the calculated values are a bit higher than the experimental values. This is caused by the unavoidable aggregation of G100 at high weight percentage in the practical case, which is not considered in the model. In the case of G5/PMMA nanocomposites, the calculated results only fit the experimental data at low contents, e.g. at 0.1 wt.%, a calculated value of 2.46 GPa to be compared with an experimental value of 2.42GPa. At 5.0 wt.%, the theory overestimates the test data to 8.64 GPa. It has a much more serious aggregation degree in the matrix at high content. Moreover, based on the SEM study and the information from supplier, the diametric distribution of G5 is not uniform, there still exist some nano pieces in the GNPs, which leads to a lower aspect ratio than the as-used value.

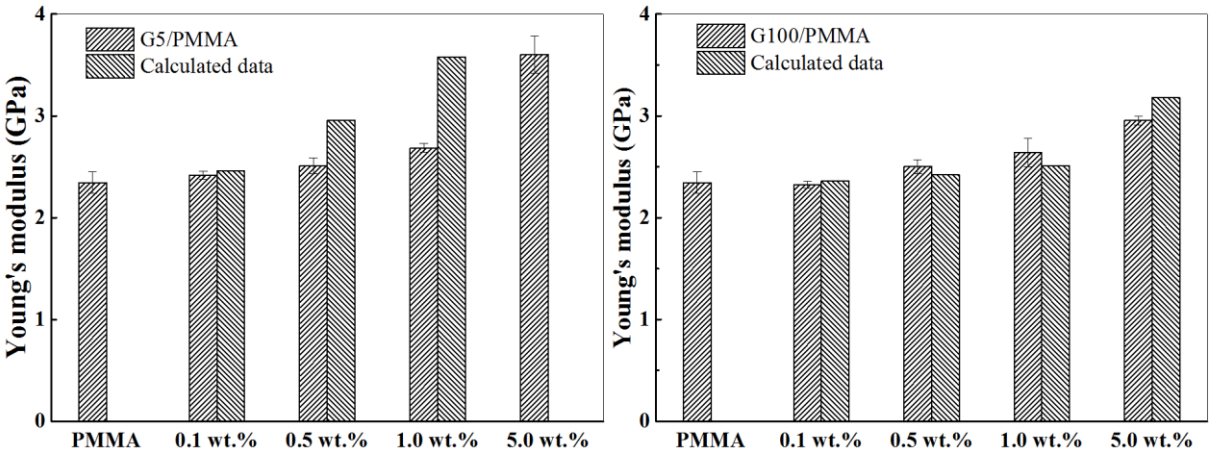

Fig 5 Comparison of Young's moduli of G5/PMMA and G100/PMMA composites with different contents with the theoretical predictions using the Halpin-Tsai model for the nanocomposite samples.

We also compare the toughness of the two GNP/PMMA composites with different contents. In order to describe the fracture behavior in a simple way, we employ the concept of volume-specific energy (*w*) in order to combine the data of strain with strength. A simple integration is used to evaluate the volume-specific energy according to the curves of stress-strain from tensile test.

The total area under the stress-strain curves in the elastic region can be used to characterize the fracture toughness. The volume-specific energy absorption can be calculated by

$$w = \int_0^{\varepsilon_0} \sigma \, d\varepsilon \qquad (6)$$

Where ε_0 is the strain at the breaking point; σ is the strength (MPa) tested by tensile test. Then, we normalize the results by dividing all the data by average value of original PMMA. The calculation results of PMMA and GNP/PMMA composites are plotted in Fig 6.

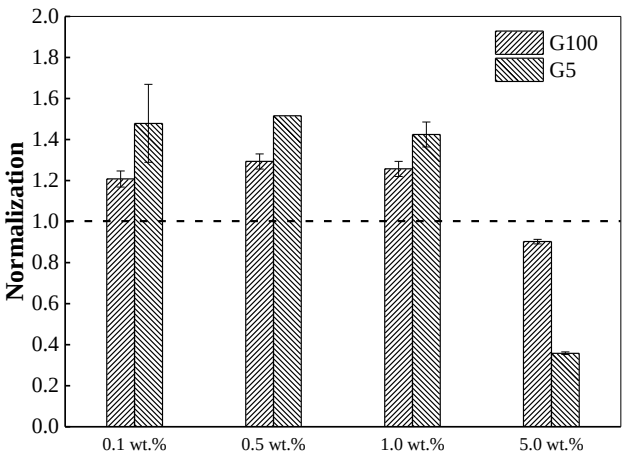

Fig 6 Variation of volume specific energy calculated by integrating the strain-strength curve.

As shown in Fig 6, the dash line represents the volume specific energy of original PMMA. Both types of composites follow the tendency that *w* increases gradually till 0.5 wt.% then has greatly decrease in 5.0 wt.%, even smaller than the pure PMMA. According to the results, it can be found that the fracture toughness could easily saturate at 0.1 wt.%, then have small increase as the content increased. The largest values for two composites both appears at 0.5 wt.%, herein, 51.6 % for G5/PMMA and 29.7 % for G100/PMMA, respectively. A widely accepted reason may be caused by more possible defects introduced into the composite due to a high content of GNPs. As shown in Fig 4, the tensile strength increases gradually as the contents increase. However, the maximum value of strain appears in the content of 0.1 wt.% instead of 5.0 wt.%, which could be explained by the same reason. In concentrations below 1.0 wt.%, the values of *w* in G5/PMMA nano-composites are higher than that of G100/PMMA nano-composites. This can be explained by the thinness of G5 which can be easy to form the network structure and improve the fracture toughness of the composite. Moreover, it is known that the mechanical property of a composite depends not only on the morphology of fillers but also the interfacial adhesion between fillers and matrix. As we mentioned in the SEM part, the interfacial adhesion of G5/PMMA is stronger than G100/PMMA composites that influences the stress transfer between GNPs and PMMA. Most results reported in the references have demonstrated that the effective stress transferring is the most important factor which contributes to the strength of two-phase composite materials. If GNPs are well bonded with PMMA, the stress transferring at the interface becomes efficient. Thus, a thinner thickness and a better adhesion with PMMA cause a high fracture toughness of G5/PMMA in all contents. Hence, by comparing the fracture toughness of GNP/PMMA composites, we find that a thinner thickness of GNP may be more appropriate for the improvement on composites' toughness.

CONCLUSIONS

According to the results in the study, the mechanical property of GNP/PMMA composites is greatly associated with the thickness of GNPs. Experimental data show that compared with G100 reinforced composite, better tensile and dynamic mechanical properties of G5 reinforced PMMA composites can be achieved due to its thinner thickness. Due to the thinness, filler network can be easier to form in the polymer matrix which possibly helps the stress transfer in the interior of the composite and thus increase its strength and fracture toughness.

ACKNOWLEGEMENT

Yu LIU thanks China Scholarship Council for the financial support. The GNPs used in this paper was purchased by GDR 3661 Polynano.

REFERENCES

1. Ramanathan T, Abdala A, Stankovich S et al. (2008) Functionalized graphene sheets for polymer nanocomposites. Nature nanotechnology 3:327-331
2. Yamamoto G, Omori M, Hashida T et al. (2008) A novel structure for carbon nanotube reinforced alumina composites with improved mechanical properties. Nanotechnology 19:315708
3. Gojny F, Wichmann M, Köpke U et al. (2004) Carbon nanotube-reinforced epoxy-composites: enhanced stiffness and fracture toughness at low nanotube content. Composites Science and Technology 64:2363-2371
4. Jiang T, Kuila T, Kim NH et al. (2013) Enhanced mechanical properties of silanized silica nanoparticle attached graphene oxide/epoxy composites. Composites Science and Technology 79:115-125
5. Wang F, Drzal LT, Qin Y et al. (2016) Size effect of graphene nanoplatelets on the morphology and mechanical behavior of glass fiber/epoxy composites. Journal of Materials Science 51:3337-3348
6. Stankovich S, Dikin DA, Dommett GHB et al. (2006) Graphene-based composite materials. Nature 442:282-286
7. Geim AK, Novoselov KS (2007) The rise of graphene. Nat Mater 6:183-191
8. Novoselov KS, Falko VI, Colombo L et al. (2012) A roadmap for graphene. Nature 490:192-200
9. Shao Y, Wang J, Wu H et al. (2010) Graphene based electrochemical sensors and biosensors: a review. Electroanalysis 22:1027-1036
10. Liu C, Yu Z, Neff D et al. (2010) Graphene-based supercapacitor with an ultrahigh energy density. Nano letters 10:4863-4868
11. Liu Y, Zhong H, Qin Y et al. (2016) Non-covalent hydrophilization of reduced graphene oxide used as a paclitaxel vehicle. RSC Advances 6:30184-30193
12. Shen J, Hu Y, Li C et al. (2009) Synthesis of amphiphilic graphene nanoplatelets. small 5:82-85
13. Stankovich S, Dikin DA, Piner RD et al. (2007) Synthesis of graphene-based nanosheets via chemical reduction of exfoliated graphite oxide. Carbon 45:1558-1565
14. Rafiee MA, Rafiee J, Srivastava I et al. (2010) Fracture and fatigue in graphene nanocomposites. small 6:179-183
15. Balandin AA (2011) Thermal properties of graphene and nanostructured carbon materials. Nature materials 10:569-581
16. Vallés C, Abdelkader AM, Young RJ et al. (2015) The effect of flake diameter on the reinforcement of few-layer graphene–PMMA composites. Composites Science and Technology 111:17-22
17. Herbert E, Oliver W, Pharr G (2008) Nanoindentation and the dynamic characterization of viscoelastic solids. Journal of Physics D: Applied Physics 41:074021
18. Rafiee MA, Rafiee J, Wang Z et al. (2009) Enhanced Mechanical Properties of Nanocomposites at Low Graphene Content. ACS Nano 3:3884-3890

19. Affdl J, Kardos J (1976) The Halpin‐Tsai equations: a review. Polymer Engineering & Science 16:344-352

20. Wang X, Xing W, Zhang P et al. (2012) Covalent functionalization of graphene with organosilane and its use as a reinforcement in epoxy composites. Composites Science and Technology 72:737-743

Captions

Fig 1 SEM images of G5 (A) and G100 (B) and the fracture surfaces of G5/PMMA (C) and G100/PMMA (D) compositeswith 5.0 wt.%.

Fig 2 Temperature dependence of storage modulus for (a) G5/PMMA and (b) G100/PMMA composites with four contents: 0.1 wt.%, 0.5 wt.%, 1.0 wt.% and 5.0 wt.%, respectively.

Fig 3 Temperature dependence of loss modulus E" for G5/PMMA and G100/PMMA composites with four contents: 0.1 wt.%, 0.5 wt.%, 1.0 wt.% and 5.0 wt.%, respectively.

Fig 4.Mechanical properties of G5/PMMA (A) and G100/PMMA (B) calculated by stress-strain curves.

Fig 5 Comparison of Young's moduli of G5/PMMA and G100/PMMA composites with different contents with the theoretical predictions using the Halpin-Tsai model for the nanocomposite samples.

Fig 6 Variation of volume specific energy calculated by integrating the strain-strength curve.

Table 1. Tg values for two kinds of GNP/PMMA composites with different contents tested by DMA method.